High Mobility of Carboxyl-Terminal Region of Bacterial Chemotaxis Phosphatase CheZ Is Diminished upon Binding Divalent Cation or CheY-P Substrate[†]

Ruth E. Silversmith[‡]

Department of Microbiology and Immunology, University of North Carolina, Chapel Hill, North Carolina 27599-7290

Received January 27, 2005; Revised Manuscript Received March 22, 2005

ABSTRACT: In *Escherichia coli* chemotaxis, the CheZ phosphatase catalyzes the removal of the phosphoryl group from the signaling molecule, CheY. The cocrystal structure of CheZ with CheY·BeF_3^-·Mg^{2+} (a stable analogue of CheY-P) revealed that CheZ is a homodimer with a multidomain, nonglobular structure. To explore the effects of CheZ/CheY complex formation on CheZ structure, the rotational dynamics of the different structural domains of CheZ [the four-helix bundle, the N-terminal helix, the C-terminal helix, and the putative disordered linker between the C-terminal helix and the bundle] were evaluated. To monitor dynamics of the different regions, fluorescein probes were covalently attached at various locations on CheZ through reaction with engineered cysteine residues and the rotational behavior of the fluoresceinated derivatives were assessed using steady state fluorescence anisotropy. Anisotropy measurements at various solution viscosities (Perrin plot analysis) demonstrated large differences in global rotational motion for fluorophores located on different regions. Rotational correlation times for probes located on the four-helix bundle and the N-terminal helix agreed well with theoretical values predicted for a protein the size and shape of the four-helix bundle. However, the rotational correlation times of probes located on the linker and the C-terminal helix were 8−20× lower, indicating rapid motion independent of the bundle. The anisotropies of probes located on the linker and the C-terminal helix increased in the presence of divalent cation (Mg^{2+}, Ca^{2+}, or Mn^{2+}) in a saturable fashion, consistent with a binding event ($K_d \sim 1-4$ mM) that results in decreased mobility. The anisotropies of probes located on the C-terminal helix and the C-terminal portion of the linker increased further as a result of binding CheY-P. In light of the recently available structural data and the high independent mobility of the C-terminus demonstrated here, we interpret the CheY-P-dependent increase in anisotropy to be a consequence of decreased mobility of the C-terminal region due to binding interactions with CheY-P, and not to the formation of higher order aggregates of the $CheZ_2$(CheY-P)$_2$ complex.

CheY, a signaling molecule in the two-component regulatory system that governs chemotaxis in *Escherichia coli*, functions as a key link between extracellular chemical information and cellular swimming behavior [see refs *1*−*3* for recent reviews of chemotaxis in *E. coli* and *Salmonella enterica* serovar Typhimurium (*S. enterica*)]. CheY is a freely diffusible cytoplasmic protein whose activity is regulated by phosphorylation at Asp57. CheY receives its phosphoryl group from the CheA kinase, which is associated with the cytoplasmic region of transmembrane receptors and whose autophosphorylation activity (using ATP) is regulated by attractant or repellent molecules bound to the extracellular portion of the receptors. CheY-P binds to the base of the flagella inducing clockwise flagellar rotation, which causes cell tumbling and reorientation of swimming direction. Although CheY has an intrinsic autodephosphorylation activity, it is too slow for the rapid information flow which occurs in chemotaxis (*4*) and the CheZ phosphatase provides the means for rapid dephosphorylation of CheY. CheZ is essential for chemotaxis in *E. coli*, and the *cheZ* gene has been found in the genomes of thirty bacterial species to date. Organisms whose genome does not encode CheZ presumably have alternate mechanisms for rapid dephosphorylation of CheY, such as an additional CheY that acts as a phosphate sink (*5*) or the presence of a different phosphatase (*6*, *7*).

In recent years, considerable progress has been made in elucidating the nature of the interaction between CheZ and CheY-P and the mechanism of CheZ-mediated dephosphorylation. The cocrystal structure of CheZ bound to CheY·BeF_3^- (a stable analogue of CheY-P) and Mg^{2+} (*8*) revealed the CheZ dimer to have a multidomain, nonglobular structure (Figure 1). The largest domain is an elongated (110 Å) four-helix bundle containing a single long helical hairpin from each monomer (residues 35−168). Extending from the "bottom" of the bundle (opposite the hairpin turns) are two additional nonglobular regions associated with each monomer. The N-terminal region (residues 1−34) forms an additional helix ("N-helix") which protrudes from the bundle at an angle of about 100°. The C-terminus of each monomer has two regions. Residues 169−199 have been proposed to comprise a disordered linker, on the basis of the absence of this stretch of residues from the crystal structure (*8*), susceptibility to proteolytic cleavage (*9*, *10*), and lack of sequence or length homology in CheZ sequences from

[†] Supported by NIH Research Grant R01 GM 050860 to Robert B. Bourret.

[‡] E-mail: silversr@med.unc.edu. Phone: 919-966-2679. Fax: 919-962-8103.

10.1021/bi0501636 CCC: $30.25
Published on Web 05/03/2005

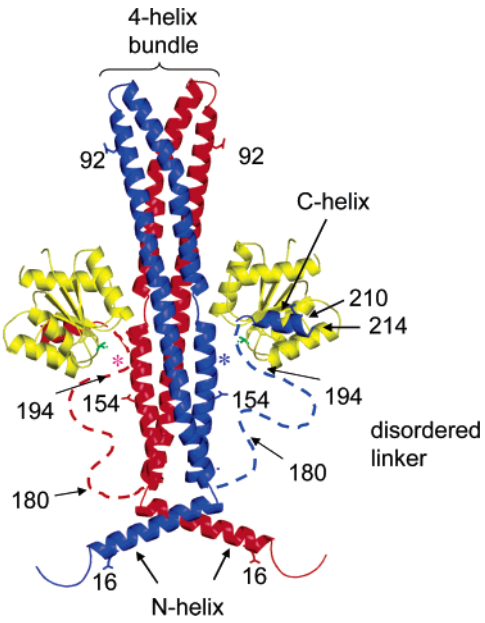

FIGURE 1: Ribbon model of the CheZ/CheY·BeF_3^-·Mg^{2+} complex (PDB 1KMI). The two CheZ chains are blue and red, and CheY is yellow. The BeF_3^- anion is displayed as a green ball-and-stick model and marks the CheY active site. The four structural regions and the sites of cysteine substitutions are indicated. The linkers are represented by dashed lines. The asterisk marks the location of the critical CheZ catalytic residue, Gln147.

different organisms (*9*). The extreme C-terminus of CheZ, residues 200−214, forms a helix in the cocrystal structure ("C-helix") which interacts with CheY·BeF_3^-·Mg^{2+}.

$CheZ_2$ has two identical binding sites for CheY-P, and each binding site contains two independent interaction surfaces between the proteins. In addition to the C-helix, a region about midway down the four-helix bundle interacts with the active site region of CheY placing the conserved CheZ catalytic residue, Gln147, in close proximity to the phosphoryl group on CheY (Figure 1) (*8*). Whereas the CheZ·CheY·BeF_3^-·Mg^{2+} structure was informative in elucidating the CheY/CheZ interaction and dephosphorylation mechanism, it is still not known what effect CheY/CheZ complex formation has on the structures of the individual proteins. The structure of uncomplexed CheZ has not yet been solved, and the electron density for CheY·BeF_3^-·Mg^{2+} in the cocrystal structure was of insufficient resolution to evaluate conformational details (*8*).

In an effort to explore the effects of CheZ/CheY complex formation on CheZ structure, we investigated the rotational dynamics of the different structural domains of CheZ under various experimental conditions. To monitor dynamics of the different regions, a fluorescein maleimide probe was placed at various locations through reaction with engineered cysteine residues. Rotational behaviors of the fluoresceinated derivatives were assessed with steady state fluorescence anisotropy. The anisotropy results demonstrated that both the linker and the C-helix exhibited high mobility that represented rapid motion independent of the global rotation of the four-helix bundle and the N-helix. The motion of portions of the linker/C-helix region was diminished by the presence of divalent cation and further by binding CheY-P. The results also allowed reevaluation of anisotropy data generated before the CheZ structural data was available.

EXPERIMENTAL PROCEDURES

Mutagenesis and Protein Purification. Site directed mutagenesis of *cheZ* was carried out using the Quikchange mutagenesis kit (Stratagene) to make *cheZ* alleles encoding CheZ D16C,[1] Q92C, D154C, R180C, S194C, D210C, and F214C. There are no cysteine residues in the wild-type CheZ sequence so all of the mutants encode CheZ variants with single cysteine substitutions. The pRS3 plasmid (pRBB40 with the inadvertent CheZ E134K mutation (*9*) corrected to Glu134) was used as the template for the mutagenesis. The mutant plasmids were transformed into the Δ*cheZ* strain, KO642*recA* (*11*) for overexpression and purification of CheZ. The CheZ cysteine substitution mutants were purified as described (*12*) with the addition of 2 mM DTT present throughout the process. A final ion exchange step was added using a MonoQ column (Amersham Biosciences) with a 0−500 mM NaCl gradient for elution (buffer was 50 mM Tris pH 7.5, 0.5 mM EDTA, 10% glycerol, 2 mM DTT). The MonoQ was effective in separation of full length $CheZ_2$ from $(CheZ_{1-181})_2$ and CheZ·$CheZ_{1-181}$ which were often detectable after execution of the standard purification protocol. Fractions from the MonoQ column were supplemented with 0.5 mM of the reducing agent, TCEP·HCl (Pierce), and stored at −20 °C. CheZ was quantitated by absorbance at 280 nm (ϵ = 16 700 M^{-1} cm^{-1}) (*12*).

Swarming Motility. Chemotactic swarming of strains containing CheZ cysteine substitution mutants were assessed by stabbing fresh colonies onto motility plates (0.3% w/v agar in tryptone broth) and incubation at 30 °C, as described (*13*).

Fluorescent Labeling. Fluorescein maleimide (Molecular Probes) was freshly prepared as a concentrated stock solution in DMSO and quantitated by absorbance at 493 nm (ϵ = 83 000 M^{-1} cm^{-1}). For high labeling efficiency (fluorescein:cysteine ratios between 0.7 and 0.9), CheZ (60−250 μM) in MonoQ elution buffer (50 mM Tris, pH 7.5, 0.5 mM EDTA, 10% glycerol, ∼250 mM NaCl, 0.5 mM TCEP·HCl) was mixed with a 20× molar excess of fluorescein maleimide, and incubated in the dark for 30 min at room temperature. The reaction mix was quenched with excess DTT (10 mM) and gel filtered (G-75 Sephadex, Amersham Pharmacia) in 50 mM Tris, pH 7.5, 0.5 mM EDTA, 2 mM DTT, 10% glycerol, which cleanly separated the fluoresceinated protein from unreacted fluorescein maleimide. The pooled sample was dialyzed overnight at 4 °C against the same buffer. To make derivatives with lower fluorescein:CheZ ratios, CheZ was transferred into 50 mM Hepes, pH 7.0, 1.0 mM TCEP·HCl and brought to a concentration of 100 μM. Fluorescein maleimide was added at several different final concentrations (10−50 μM). After 5 min at room temperature, the reactions were quenched with 10 mM DTT. Labeled protein was chromatographed on G-75 Sephadex in 50 mM Hepes, pH 7.0, 1.0 mM TCEP·HCl and fluoresceinated-CheZ was pooled. Labeled proteins were stored in aliquots at −70 °C.

[1] Abbreviations: CheZ D16C, CheZ with the wild-type aspartate at position 16 changed to a cysteine (this format is used to identify mutants throughout the manuscript); fl-CheZ, fluoresceinated CheZ; TCEP·HCl, Tris (2-carboxyethyl)-phosphine hydrochloride; DTT, dithiothreitol; EDTA, ethylenediaminetetraacetate; DMSO, dimethyl sulfoxide; ϕ, rotational correlation time; A_0, limiting anisotropy; η, viscosity; τ, fluorescence lifetime; PDB, Protein Data Bank.

Determination of Labeling Efficiency and Mass Spectral Analysis of Labeled CheZs. Protein concentrations of derivatized proteins were determined using the Biorad protein assay (based on the Bradford method) with unlabeled CheZ as a standard. The fluorescein concentration was determined by dilution into 50 mM Tris, pH 9.0 and measurement of the absorbance at 493 nm ($\epsilon = 83\,000\ M^{-1}\ cm^{-1}$). Electrospray mass spectrometry (Fisions-VG Quattro BQ triple quadropole) analysis of representative preparations of fluoresceinated proteins with high fluorescein:protein ratios showed the dominant mass consistent with single labeling with fluorescein maleimide with the addition of a water molecule to the maleimide ring (*14*). There was no detectable multiply labeled protein and little or no detectable unlabeled protein.

Fluorescein Labeling of CheZ Peptide. The peptide corresponding to the 19 carboxyl-terminal residues of CheZ D210C (AGVVASQDQVDDLLCSLGF) was synthesized by the University of North Carolina Microprotein Sequencing and Peptide Synthesis Facility. The peptide (2 mg in 200 μL of Hepes pH 7.0, 1 mM TCEP·HCl) was incubated with a 5× molar excess of fluorescein maleimide for 1 h at room temperature. Labeled peptide was separated from free reagent by gel filtration chromatography (Superdex 75, Amersham Biosciences) followed by reverse phase HPLC (Agilent Eclipse XDB-C8 column) with a gradient of 36−63% acetonitrile in 0.1% trifluoroacetic acid. Fractions containing visible fluorescein were lyophilized and analyzed by electrospray mass spectrometry using a Bio-TOF II (Bruker Daltronics ESI-TOF). The labeled peptide was identified by the presence of a mass corresponding to the monosubstituted peptide with an additional 17 Da, consistent with the opening of the maleimide ring with a molecule of water (*14*), as observed with the full length CheZ. The mass spectrum of the sample containing labeled peptide showed no detectable unlabeled peptide or free fluorescein maleimide.

Fluorescence Anisotropy Measurements. A Perkin-Elmer LS-50B spectrofluorimeter equipped with magnetic stir mechanism and thermostated cuvette holder was used. Cuvette temperature control was with a circulating water bath and was maintained at 20.0 ± 0.3 °C. Excitation and emission were set at 480 and 520 nm, respectively, and slit widths were 7.5 nm. For measurements using fluoresceinated CheZ with low labeling ratios, the slit widths were increased to enhance the signal of the individual emission intensities (I_{VH} and I_{VV}). The instrument software (FLWIN) provided automatic polarizer control and calculation of anisotropy, taking into account an instrumental *G*-factor (a correction factor for differential sensitivity to vertically and horizontally polarized light) which was measured by the manufacturers. Anisotropy values were generated about every 30 s. Six consecutive readings were made for each sample condition and the values averaged. For titration of CheZ samples with divalent cations, small volumes of the metal ion were sequentially added to the fluoresceinated CheZ (0.2 μM in 50 mM Hepes, pH 8.0) with constant stirring. For titration with CheY N59R-P, CheY N59R was incrementally added to CheZ (0.2 μM in 50 mM Hepes, pH 8.0, 10 mM $MgCl_2$, 19 mM acetyl phosphate). To analyze the effect of divalent metal ion on anisotropy, the data were plotted as A/A_{apo} (observed anisotropy divided by the anisotropy in the absence of divalent cation) versus metal ion concentration, [Me^{2+}]. The curves were fit to the following simple hyperbolic binding model using Kaleidograph software: $A/A_{apo} = \{(A_\infty/A_{apo}K_a[Me^{2+}]) + 1\}/(1 + K_a[Me^{2+}])$, where A_∞ is the maximal change in anisotropy, and K_a is the apparent association constant between the divalent cation and CheZ.

Perrin Plot Analysis and Calculation of Hydrodynamic Parameters. Anisotropy values have contributions from both the global rotation of the protein to which the fluorophore is attached and the localized rotation of the fluorophore. Perrin plot analysis was used to determine hydrodynamic parameters describing both types of rotational motion for the fl-CheZs. The Perrin relationship (*15*) states that

$$1/A = 1/A_0 + \tau kT/\eta V_h A_0 \quad (1)$$

where A is the measured anisotropy, A_0 is the limiting anisotropy (the residual anisotropy of the probe when the protein is "frozen" in solution), τ is the fluorescence lifetime of the probe, k is Boltzmann's constant, T is temperature in kelvins, η is solution viscosity, and V_h is the hydrodynamic volume of the protein to which the fluorophore is attached. The value of V_h reflects the rotational dynamics of the protein. Experimentally, the anisotropy is measured as a function of either temperature or viscosity. The Perrin relationship states that plots of $1/A$ versus T/η are linear with the y-intercept equal to $1/A_0$ and slope equal to $\tau k/V_h A_0$.

For our analysis, the anisotropy was measured at various solution viscosities. Samples were prepared by addition of individual fl-CheZ (final concentration 0.2 μM) to solutions containing various concentrations of sucrose [0−30% (w/w)]. Viscosities were obtained from standard tables summarizing physical properties of aqueous sucrose solutions (*16*). Unless otherwise noted, the standard buffer was 25 mM Hepes, pH 8.0, 0.1 mM TCEP·HCl. Samples were incubated at room temperature in the dark for 2 h. Temperature equilibration of samples at 20 °C was allowed for 3 min in the cuvette holder before anisotropy readings were taken. The data were plotted as $1/A$ versus T/η, and A_0 and V_h were determined from the y-intercept and slope as stated above. The fluorescence lifetime (τ) of fluorescein was assumed to be 4 ns (*15*). An additional hydrodynamic parameter, the rotational correlation time (ϕ) at 0.01 P (poise) (viscosity of water at 20 °C) and 20 °C, was calculated from V_h using the relationship (*15*)

$$\phi = \eta V_h/kT \quad (2)$$

The rotational correlation time is the decay constant for the exponential decay of fluorescence anisotropy. The higher the ϕ value, the slower the rotation, the larger the molecule. The ϕ value must be comparable to the fluorescence lifetime of the fluorophore in order to obtain information about rotational dynamics using fluorescence anisotropy.

Prediction of Rotational Parameters Using HYDROPRO Software. HYDROPRO (*17*) is a public domain program which predicts hydrodynamic parameters from an input protein PDB file using a bead shell method to model the surface of the protein. The software was downloaded from [http://leonardo.fcu.um.es/macromol/programs/programs.html].

RESULTS

Preparation and Initial Characterization of Fluoresceinated CheZs. The CheZ·CheY·BeF_3^-·Mg^2 cocrystal structure revealed four structural regions within the CheZ homodimer: the N-helix (residues 1−34), the four-helix bundle (residues 35−168), the linker (residues 169−199), and the C-helix (residues 200−214). To spectroscopically probe the rotational dynamics of these regions, we covalently linked fluorescein maleimide to various CheZ mutant proteins that contained single cysteine substitutions. Cysteines were substituted for Asp16 (located on the N-helix), Gln92 and Asp154 (four-helix bundle), Arg180 and Ser194 (linker), and Asp210 and Phe214 (C-helix) (Figure 1). All of the residues substituted with cysteine had no implicit functional role, on the basis of CheZ/CheY interactions revealed by the cocrystal structure, published biochemical or genetic analysis, and lack of sequence conservation in alignments of CheZ sequences from 30 bacterial species (data not shown). Placement of cysteine at Phe214 was of particular interest for direct comparison to published fluorescence anisotropy measurements using fluorescein maleimide-labeled CheZ F214C from *S. enterica* (*18*). All of the single cysteine substitutions conferred wild-type levels of chemotactic swarming when expressed in the CheZ-deleted strain, K0642*recA* (data not shown), confirming that the ability of the mutants to dephosphorylate CheY was not affected by the substitutions.

All of the single cysteine CheZs reacted readily with fluorescein maleimide. The first set of derivatized proteins were labeled under conditions that gave high degrees of labeling (∼0.7−0.9 mol of fluorescein/mol of CheZ). Initial anisotropy measurements (measured in 25 mM Hepes, pH 8.0, 0.1 mM TCEP·HCl) for the different derivatives varied significantly with values (in order of increasing anisotropy) of 0.053 (fl-CheZ F214C), 0.071 (fl-CheZ S194C), 0.078 (fl-CheZ R180C), 0.083 (fl-CheZ D210C), 0.113 (fl-CheZ Q92C), 0.122 (fl-CheZ D16C), and 0.161 (fl-CheZ R154C). Anisotropy measurements have a high degree of precision, and all the aforementioned values had errors of no more than ±0.002. Anisotropy values approaching zero are expected if the fluorescein rotates rapidly relative to its fluorescence lifetime, such as free fluorescein in a low viscosity solvent. The upper limit for anisotropy of fluorescein is about 0.35 (*15*). Within this theoretical range of anisotropy values, the measured anisotropy is largely dependent on the rotational motion of the fluorophore.

Possible Influence of homo-FRET on Anisotropy Values. Whereas the magnitude of the anisotropy is mainly dependent on rotational motion, another factor which might affect values here is resonance energy transfer between two fluorescein groups located on the same CheZ dimer. This phenomenon, "homo-FRET", decreases anisotropy values because the orientations of the acceptor fluoresceins are randomized (*15*, *19*). In CheZ, the intradimer distances for several of the labeled residues are comparable to the Förster critical distance for fluorescein/fluorescein energy transfer [(50 Å (*19*)]. To assess the possible influence of homo-FRET, the anisotropies of CheZ derivatives with lower labeling ratios were measured (Figure 2). Lower labeling ratios would decrease the proportion of doubly labeled dimers and diminish any contribution from homo-FRET. For CheZ derivatives labeled on the four-helix bundle (positions 92 and 154), N-helix (position 16), and C-helix (positions 210 and 214), there was a modest increase in anisotropy as labeling ratios were lowered, consistent with a contribution from homo-FRET (Figure 2). The CheZs labeled on the linker (position 180 or 194) showed little or no sensitivity to labeling ratio. The occurrence of homo-FRET is not unexpected for CheZs derivatized at positions 16, 92, or 154 as these residues are separated by their identical homologue by 36, 28, and 23 Å, respectively, within CheY·BeF_3^-·Mg^{2+} (*8*). However, the possible occurrence of homo-FRET for the C-helix derivatives (210 and 214) was unexpected but may indicate that the C-helices are, on average, in closer proximity in the absence of CheY-P than in its presence (50−70 Å). In any case, the magnitudes of the effects of homo-FRET on any of the fl-CheZs were small relative to the differences in anisotropies between the derivatives. Therefore, the anisotropies largely reflect different rotational mobilities of fluorescein located at different regions of CheZ. The rest of the experiments used fl-CheZs with high fl:CheZ ratios.

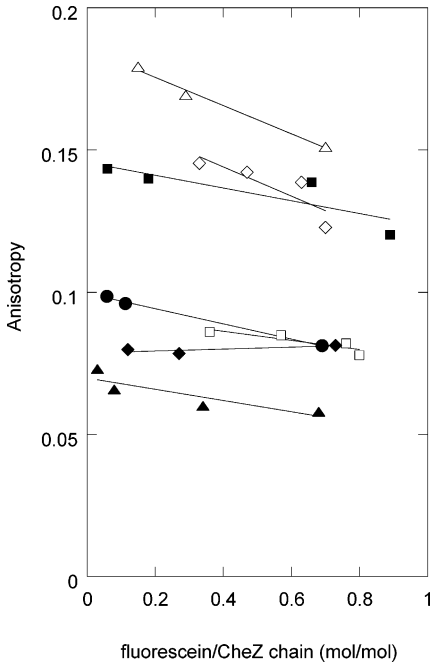

FIGURE 2: Anisotropy of fl-CheZs with varying fluorescein/CheZ monomer ratios. The anisotropies are shown for derivatives with fluorescein at position 16 (◇), 92 (■), 154 (△), 180 (□), 194 (◆), 210 (●), and 214 (▲).

Delineation of Global versus Localized Rotation Using Perrin Plots. Anisotropy values have contributions from both localized motion of the fluorophore and global rotation of the protein to which the probe is attached, which is of primary interest. To determine the relative contributions of global and localized motion to the anisotropies of the various fluoresceinated CheZ proteins, Perrin plot analysis was used. Plots of $(\text{anisotropy})^{-1}$ as a function of temperature divided by solution viscosity for each fluoresceinated CheZ were linear, as expected (Figure 3). The set of fl-CheZ derivatives showed little variation in *y*-intercept values reflecting a narrow range of limiting anisotropies, with $A_0 = 0.17 \pm 0.03$. This value is typical for fluorescein linked to a protein (*15*). There was no apparent correlation between A_0 and the structural region to which the probe was attached (Table 1). The similar values of A_0 probably reflect the fact that all of

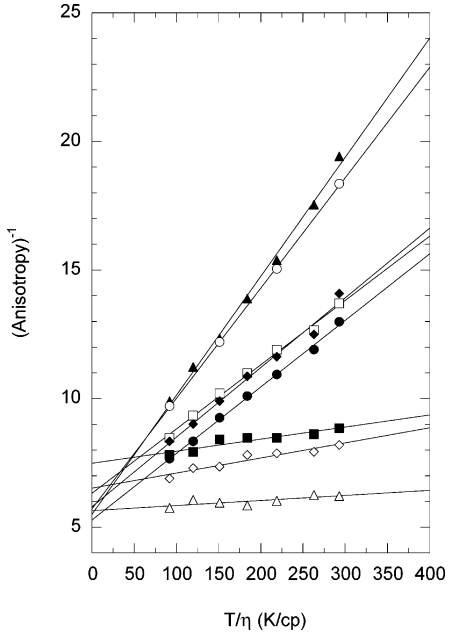

FIGURE 3: Perrin plots for fluoresceinated CheZs measured in 25 mM Hepes, pH 8.0, 0.1 mM TCEP·HCl. Data are shown for derivatives with fluorescein at position 16 (◇), 92 (■), 154 (△), 180 (□), 194 (◆), 210 (●), 214 (▲) in CheZ, and fl-CheZ D210C$_{196-214}$ (○).

the labeled cysteines were solvent exposed and used the same maleimide linkage.

In contrast to the similar *y*-intercepts, there was significant variation in slopes for the CheZ derivatives which translated into marked differences in rotational correlation times (ϕ) (Table 1, values for standard HEPES). Rotational correlation times for probes located on the same structural region were similar, as would be expected if the behavior was reflective of the rotational behavior of the structural region. The rotational behavior of the derivatives fell into several groups (Table 1). The fl-CheZs labeled on the four-helix bundle (positions 92 and 154) displayed low slopes in Perrin plots (Figure 3), which gave ϕ values of 30 ± 10 ns. The low slope values resulted in a relatively large error when values from independent experiments were compared, and we conclude that this method cannot distinguish ϕ values greater than about 20 ns for proteins labeled with fluorescein. This high ϕ value (>20 ns) for both probes located on the four-helix bundle correlates with theoretical values predicted for a protein the size and shape of CheZ. The HYDROPRO program (*17*) predicted a correlation time of 52 ns for the four-helix bundle and N-helix regions of CheZ alone. Furthermore, analysis of measurements from many proteins (*15*) has shown that rotational correlation times deduced from Perrin plots are about 2-fold the value predicted if the protein was an anhydrous sphere of the same molecular weight. An anhydrous sphere with a molecular weight of 48 000 (mass of the CheZ dimer) would have a correlation time of about 14 ns (*15*), predicting a value of 28 ns measured by fluorescence anisotropy (Table 1). A rotational correlation time of >20 ns is significantly larger than the fluorescence lifetime of fluorescein (4 ns). Therefore, anisotropy measurements using fluorescein would not be expected to be sensitive to changes in the global motions of the CheZ four-helix bundle, such as self-association or association with another protein, but would require a longer lifetime probe.

In contrast to the fl-CheZs labeled on the four-helix bundle, the CheZs labeled on the linker or the C-helix gave high slopes in the Perrin plot that correlated to rotational correlation times 8−20 times smaller (Table 1). fl-CheZ D210C (C-helix), fl-CheZ R180C (linker), and fl-CheZS194C (linker) displayed similar rotational correlation times of about 3−4 ns, an order of magnitude smaller than the derivatives labeled on the four-helix bundle. Fl-CheZ F214C, located at the extreme C-terminus, displayed even faster rotational hydrodynamics (ϕ = 1.7 ns). Notably, this derivative was not measurably different from fl-CheZ D210C$_{196-214}$, a peptide of only 19 amino acids (Figure 3, Table 1). Therefore, the linker and the C-helix regions of CheZ rotate with dynamics much faster than would be expected if they were limited by the rotation of the four-helix bundle and instead rotate like a peptide of similar size. Rotation of the linker and C-terminal portions of CheZ independently of the bundle indicates little interaction between these regions and the bundle. The extreme mobility of the fl-CheZ F214C relative to derivatives at positions 210, 194, and 180 may reflect the extra degree of freedom gained from location at the extreme C-terminus.

Finally, CheZ labeled on the N-helix at position 16 had an intermediate correlation time (15 ns), measurably faster than derivatives labeled on the four-helix bundle but markedly slower than the linker and C-helix derivatives. Because the N-helix is similar in size to the C-helix and fl-CheZ$_{196-214}$, independent rotation (as was seen with the C-helix) would be expected to give similarly low rotational correlation times. Therefore, unlike the linker and C-helix, the N-helix rotates predominantly as part of the bundle, but has some limited independent motion.

Effects of Divalent Cation on Rotational Dynamics. The CheZ-dependent dephosphorylation of CheY has an absolute requirement for divalent cation, requiring that Mg^{2+} be present in experiments evaluating CheZ/CheY-P interactions. It was thus necessary to explore the effects, if any, of Mg^{2+} alone on the anisotropies of the various CheZ derivatives. The presence of $MgCl_2$ affected the anisotropies of the derivatives differentially (Figure 4a). Incremental addition of $MgCl_2$ to both linker derivatives (positions 180 and 194) and both C-helix derivatives (positions 210 and 214) resulted in progressive increases in anisotropy which eventually approached saturation (Figure 4a). In contrast, identical titrations of CheZ labeled on the four-helix bundle (92 and 154) and the N-helix (16) did not give a significant (>0.005) or consistent change in anisotropy (Figure 4a). The data for fl-CheZs labeled at positions 194, 210, and 214 were fit to a simple binding model with K_d values of 3.5 mM (position 214), 1.3 mM (position 210), and 2.6 mM (position 194) and correlation coefficients >0.99 (data not shown).

Experiments to further characterize the effect of $MgCl_2$ used fl-CheZ D210C, which had the highest apparent affinity for Mg^{2+}. The anisotropy change upon titration with $MgCl_2$ did not occur in the presence of excess EDTA (Figure 4b), indicating that the effect was due to the presence of Mg^{2+} and not Cl^-. Titration of fl-CheZ D210C$_{196-214}$ with $MgCl_2$ also did not change the anisotropy (Figure 4b). Two other divalent metal salts tested, $CaCl_2$ and $MnCl_2$, also caused progressive increases in anisotropy which eventually approached saturation (Figure 4b). The data for all three metals were fit to a simple binding model (correlation coefficients

Table 1: Hydrodynamic Parameters Derived from Perrin Plots of Flouresceinated CheZs under Various Conditions

location of flourescein		y-intercept[a]	slope[a]	ϕ^a	ϕ^b (Mg, KCl)	ϕ^c (Y/Z)
residue	domain	(=$1/A_0$)	(cP/K $\times 10^3$)	(ns)	(ns)	(ns)
16	N-helix	6.3 ± 0.3[d]	5.8 ± 0.0	14.8 ± 0.4	18	12
92	bundle	7.3 ± 0.3	3.6 ± 0.7	30 ± 11	nd[e]	nd
154	bundle	5.5 ± 0.2	2.5 ± 0.4	32 ± 11	34	25
180	linker	6.2 ± 0.2	23 ± 1	3.7 ± 0.3	4.4	4.8
194	linker	5.8 ± 0.0	25 ± 2	3.3 ± 0.5	3.6	11
210	C-helix	5.1 ± 0.2	23 ± 2	3.0 ± 0.3	6.4	7.3
214	C-helix	5.4 ± 0.1	43 ± 2	1.7 ± 0.2	2.7	9.4
"210"	CheZ $D210C_{196-214}$ peptide	5.7	43	1.7	nd	nd

[a] Measurements were in 25 mM Hepes, pH 8.0, 0.1 mM TCEP·HCl. [b] Measurements were in 25 mM Hepes, pH 8.0, 0.1 mM TCEP·HCl, 1 mM $MgCl_2$, 75 mM KCl. [c] Measurements were in 25 mM Hepes, pH 8.0, 0.1 mM TCEP·HCl, 8 mM $MgCl_2$, 20 mM acetyl phosphate (Sigma) and 0.5 μM CheY N59R. [d] Values represent the average and standard deviation of two independent experiments. [e] Not determined.

>0.99) and gave K_d values of 1.3 mM (Mg^{2+}), 1.3 mM (Ca^{2+}), and 1.6 mM (Mn^{2+}) (Figure 4b). That Mg^{2+}, Mn^{2+}, and Ca^{2+} gave similar binding constants may indicate that the binding site is not highly specific. Perrin plots of fl-CheZ D210C in the presence of subsaturating (1 mM) and saturating (8 mM) Mg^{2+} (Figure 4c) demonstrated that Mg^{2+} affected the slopes and not the intercepts, consistent with an effect on the global rotation of the linker and C-helix. Finally, none of the cations affected the fluorescence intensity of fl-CheZ D210C (data not shown). Fluorescence intensity is an indicator of fluorescence lifetime, and changes in fluorescence lifetimes can artificially impact anisotropy values. Taken together, these observations are consistent with a binding event between divalent cation and CheZ with an affinity in the low millimolar range which decreases the rotational mobility of the C-terminal region. Linkage to the four-helix bundle appears to be necessary, and Mn^{2+} appears to result in a more severe loss of mobility than Mg^{2+} or Ca^{2+}.

Rotational Parameters under Physiological Mg^{2+} Concentration and Higher Ionic Strength. In light of the effect of divalent cation on the rotational motion of the C-terminal portion of CheZ, we examined how solution conditions more reflective of the physiologic environment of the cell cytoplasm affected rotational parameters. The cytoplasm of an *E. coli* cell contains about 1−2 mM free Mg^{2+} (*20*) and an ionic strength of about 150 mM (*21*), composed mainly of KCl. Increasing the KCl concentration from 0 to 70 mM resulted in a small (<0.01) increase in anisotropy for fl-CheZ D210C and had no effect on the anisotropy of fl-CheZ $D210C_{196-214}$ (data not shown). Perrin plots of the fl-CheZs in buffer containing 75 mM KCl /1 mM Mg^{2+} gave slightly higher ϕ values for the two C-helix derivatives but did not affect the ϕ values for the other derivatives (Table 1). Therefore, rapid independent motion of the C-terminal region of CheZ also occurs under conditions more reflective of the cell cytoplasm.

Effect of CheY-P on Anisotropies. CheY N59R-P binds to CheZ but is resistant to its phosphatase activity (*12*, *22*). This mutant CheY therefore provides a convenient tool to characterize binding events between CheY-P and CheZ without the necessity of considering the effect of CheZ on CheY-P concentrations (*12*). Titration of fl-CheZ F214C with CheY N59R under phosphorylating conditions resulted in progressive increases in anisotropy which saturated at about 0.2 μM CheY and an anisotropy of about 0.13 (Figure 5). This is indistinguishable from a similar titration with *S. enterica* fl-CheZ F214C (*12*) and is consistent with essentially quantitative binding of CheYN59R-P to CheZ which results in a loss of fluorescein mobility. The same titration with wild-type CheY results in a similar degree of anisotropy change but requires higher CheY concentration (*18*), because CheZ diminishes the CheY-P concentration (*12*). CheZs labeled at position 210 (also C-helix) and 194 (C-terminal region of linker) displayed similar responses to CheY-P, indicating loss of mobility for the C-helix and the portion of the linker near the helix. However, the anisotropy of fl-CheZ R180C (N-terminal region of linker) did not change, suggesting that the N-terminal region of the linker retains high mobility even in the CheZ/CheY complex. CheZ labeled on the four-helix bundle (positions 92 and 154) also did not change upon binding CheY-P. However, these fluorophores are insensitive to decreases in mobility because their rotational correlation times are already significantly higher than the fluorescence lifetime of fluorescein (see earlier discussion). The anisotropy of fl-CheZ D16C also increased upon binding CheYN59R-P. This was surprising as the N-helix is far from the CheY-P binding site and may indicate a heretofore unknown conformational change in the N-helix upon binding CheY-P. For comparison, the CheZs were also titrated with wild-type CheY complexed to BeF_3^- and Mg^{2+}. These titrations were, within experimental error, the same as the titrations for CheY N59R-P (data not shown). CheY N59R-P did not change the fluorescein intensity of most of the derivatives. The exception was fl-CheZ D210C, whose emission intensity increased by 10−15% upon binding CheY N59R-P (data not shown).

Perrin plots (Figure 6) and subsequent calculation of ϕ values (Table 1) confirmed that CheZ derivatives labeled at positions 214, 210, and 194 had ϕ values significantly higher in the CheZ/CheY N59R-P complex than in their uncomplexed state. However, the ϕ values were still measurably lower than those for CheZ D154C, implying motion faster than that of the four-helix bundle. Only fl-CheZ R180C maintained the high mobility in the CheZ/CheY complex which was comparable to motion in the absence of CheY-P.

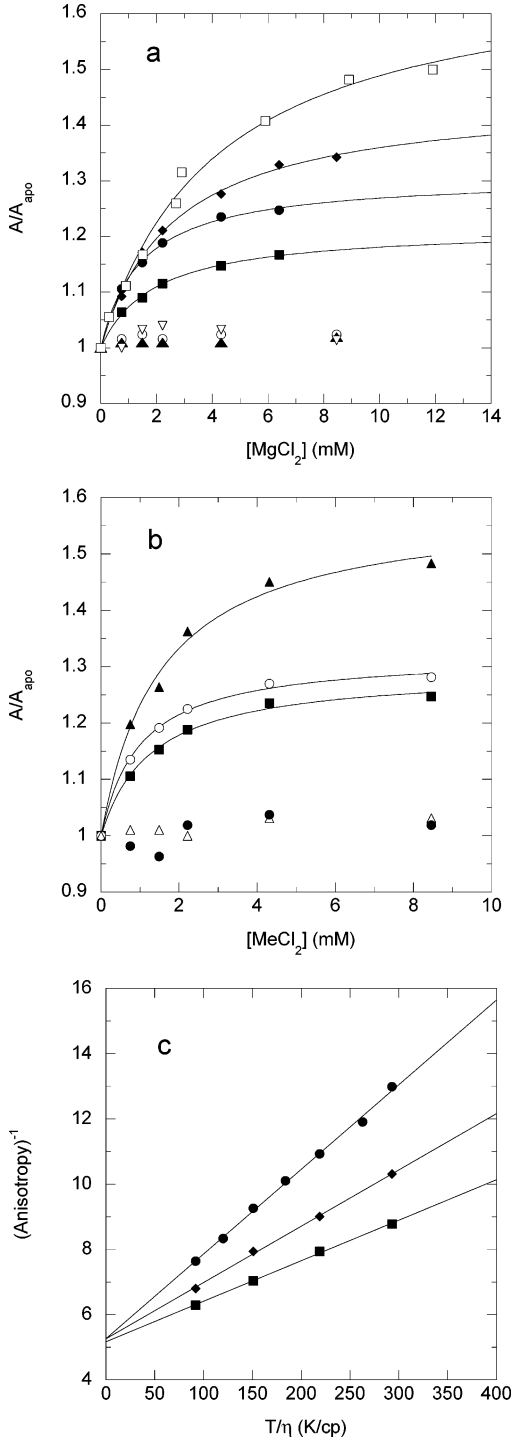

FIGURE 4: The effect of divalent cations on the anisotropies of fl-CheZs. (a) Anisotropy changes for each derivatized CheZ as a function of increasing concentration of $MgCl_2$. Anisotropy was plotted as A/A_{apo} (A_{apo} is anisotropy in the absence of metal). Data are shown for CheZ fluoresceinated at position 16 (○), 92 (▲), 154 (▽), 180 (■), 194 (◆), 210 (●), and 214 (□). Curve fits using a simple binding isotherm are shown. (b) Anisotropy changes for fl-CheZ D210C for titration with $MgCl_2$ in the absence (■) and presence (●) of 20 mM EDTA. Also shown are titrations with $CaCl_2$ (○) and $MnCl_2$ (▲). Addition of $MgCl_2$ to fl-CheZ $D210C_{196-214}$ is indicated by open triangles (△). Curve fits using a simple binding isotherm are shown [K_d values were 1.3 mM (Mg^{2+}), 1.3 (Ca^{2+}), and 1.6 mM (Mn^{2+})]. (c) Perrin plots for fl-CheZ D210C under various buffer conditions. All are in 25 mM Hepes, pH 8.0, 0.1 mM TCEP·HCl: no addition (●), 1 mM $MgCl_2$ (◆), and 8 mM $MgCl_2$ (■).

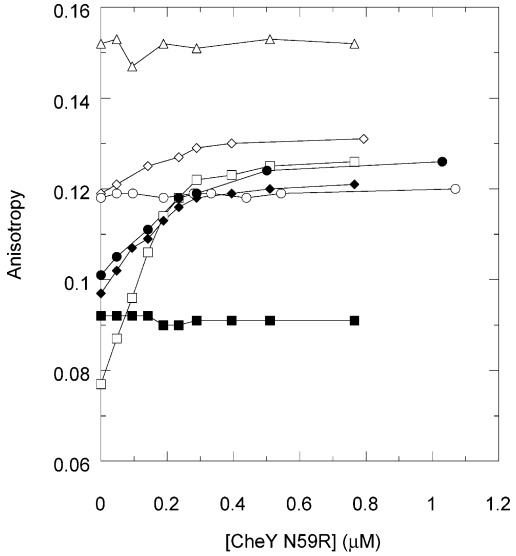

FIGURE 5: The effect of binding CheY N59R-P on the anisotropies of the fl-CheZs. CheZ was titrated with CheY N59R under conditions which should phosphorylate all of the CheY. Data are shown for derivatives with fluorescein at position 16 (◇), 92 (○), 154 (△), 180 (■), 194 (◆), 210 (●), and 214 (□).

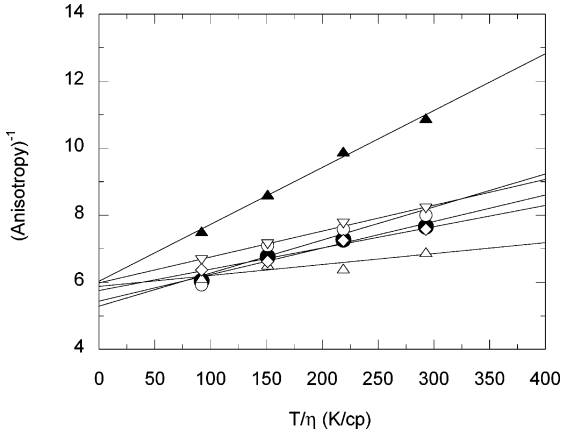

FIGURE 6: Perrin plots for fl-CheZs in the CheZ/CheY N59R-P complex. Data are shown for derivatives with fluorescein at position 16 (◇), 154 (△), 180 (▲), 194 (▽), 210 (○), and 214 (●).

DISCUSSION

Highly Mobile C-Terminus May Increase Effective Radius of CheZ for Sampling CheY-P Molecules. There is mounting evidence that, in vivo, a significant portion of CheZ is associated with the polar supramolecular sensory complex which also contains transmembrane chemoreceptors, the cytoplasmic sensor kinase CheA, and a coupling protein CheW (*23*, *24*). Recent evidence (*25*, *26*) suggests that colocalization of the CheZ phosphatase with the CheA kinase serves to maintain a constant CheY-P concentration over the length of the cell at any moment. Association of CheZ with the complex is thought to be mediated by direct interaction between the hairpin region of the CheZ four-helix bundle and CheA-short (*24*, *27*), a truncated version of CheA which comprises about one-third of the cellular CheA (*28*). Here we demonstrated that the C-terminal ~45 residues of CheZ display high rotational mobility which is largely independent of the much slower rotation of the four-helix bundle. This high mobility suggests that, in vivo, the C-terminal region

of CheZ may behave like an arm that swings independently of the anchored CheZ four-helix bundle, thereby increasing the space over which CheZ can potentially collide with CheY-P. Generation of CheY-P by the proximal CheA kinase would result in high local concentrations of both CheY-P and the CheZ C-helix, which would further increase the probability of their collision and subsequent association; the $CheZ_{196-214}$ peptide, which correlates to the CheZ C-helix, binds CheY-P with an appreciable affinity [$K_d = 26\ \mu M$ (*29*)]. Initial association of CheY-P and the C-helix would bring CheY-P into the proximity of the four-helix bundle, which would enhance the probability of interaction between the four-helix bundle and the active site of CheY, which leads to dephosphorylation. The independent mobility of the C-linker/helix region of CheZ may therefore, in essence, increase the effective radius of the CheZ dimer for sampling diffusing CheY-P molecules. This factor, along with the effects of high local concentrations of reactants, may contribute to maximization of the association rate between CheY-P and CheZ. Rapid association of CheY-P and CheZ has been observed using stopped flow fluorescence anisotropy (*30*).

The concept of the C-terminal region of CheZ as an independently swinging arm might be limited by vulnerability of such an unprotected region to intracellular proteases. A possible means of protection from proteases could be derived from transient association of the CheZ C-helix and/or linker region with the supramolecular sensory complex. One possibility is that the C-helix associates with another region of CheZ. Here we demonstrated that divalent cation (e.g. Mg^{2+}) decreased the mobility of the C-helix in the context of the full length CheZ, but did not affect the mobility of the free peptide that correlates to the CheZ C-helix. The affinity of CheZ for Mg^{2+} (1−4 mM) was comparable to the concentration of intracellular free Mg^{2+} (∼1−2 mM). Thus, it is possible that, in vivo, there could be populations of both Mg^{2+}-bound CheZ (with some association between the C-helix and the four-helix bundle that could provide protection from proteases) and Mg^{2+}-free CheZ (with the C-helix rotating freely of the bundle to optimize the chance of collision with CheY-P interaction).

Divalent Metal Effect on Anisotropy—Where Is the Metal Binding Site? There was a clear effect of the divalent metal ions Mg^{2+}, Mn^{2+}, and Ca^{2+} (all that were tested) on the anisotropies of the fl-CheZs which had the fluorescein located on the C-helix or linker. The effect appeared to reflect a binding event between metal ion and CheZ that decreased the mobility of the C-region of CheZ; the data was hyperbolic and fit well to a simple ligand binding model. Interestingly, the $CheZ{\cdot}CheY{\cdot}BeF_3^-{\cdot}Mg^{2+}$ cocrystal structure did not reveal a bound Mg^{2+} ion, aside from the Mg^{2+} bound in the CheY active site, although the crystals were grown in the presence of 10 mM $MgCl_2$. Although further experiments must be done to determine the divalent cation binding site, it may be notable that the CheZ C-helix contains highly conserved aspartate residues at positions 203, 206, and 207, which could potentially provide ligands for a Mg^{2+} ion. However, it is not known whether this stretch of residues has any helical structure when it is not bound to CheY, which might be expected to bring the residues closer together. Circular dichroism experiments did not detect α-helicity in a synthetic peptide corresponding to $CheZ_{196-214}$ in the presence or absence of 10 mM Mg^{2+} (Silversmith, unpublished result).

Insufficient Evidence for Formation of Higher Aggregates of $CheZ_2(CheY\text{-}P)_2$. We confirmed an earlier observation that CheY-P increases the fluorescence anisotropy of fluorescein maleimide-linked CheZ F214C (*18*). At the time of the original observation, the $CheZ/CheY{\cdot}BeF_3^-{\cdot}Mg^{2+}$ cocrystal structure was unavailable and the 4- to 5-fold decrease in slopes for Perrin plots for the fl-CheZ F214C/CheY-P complex relative to free fl-CheZ F214C was attributed to formation of higher aggregates of $CheZ_2(CheY\text{-}P)_2$. Here, we demonstrated that the rotational correlation times (ϕ) for fl-CheZ F214C and other CheZ derivatives labeled near the C-terminus were 8−20× shorter than expected if their rotation was limited by rotation of the four-helix bundle. Therefore, in the absence of CheY-P, the C-terminal region has rapid motion independent of the rotation of the core protein. Binding CheY-P increases ϕ of the C-terminal region to a value close to the overall rotation of the core protein. In light of the now available structural information, these observations can be most easily explained by lost mobility from anchoring the C-helix to CheY-P, as revealed by the cocrystal structure. Furthermore, fluorescence anisotropy using fluorescein as a probe is not a useful technique for determining the ability of $CheZ_2(CheY\text{-}P)_2$ to form higher aggregates, because the rotational dynamics of the four-helix bundle are already slow relative to the fluorescence lifetime of fluorescein. Any further slowing of rotation, e.g. due to aggregate formation, would not be detectable by this method.

Although fluorescence anisotropy cannot be used as positive evidence for oligomerization of the CheZ/CheY-P complex, it does not itself rule oligomerization out. There remain several observations which address the possibility of formation of higher aggregates of $CheZ_2(CheY\text{-}P)_2$. Evidence that argues against oligomerization includes the observation that the CheZ/CheY59NR-P complex elutes from an analytical gel filtration column with a mobility which is indistinguishable from that of the CheZ dimer (*12*). Evidence in support of oligomerization comes from cross-linking experiments where products of 90−200 kDa are formed upon incubation of CheZ and CheY-P (but not unphosphorylated CheY) with a bifunctional cross-linking reagent that reacts with lysine and aspartate residues (the molecular weight of $CheZ_2(CheY\text{-}P)_2$ is 76 kDa) (*18*). However, cross-linked protein complexes can occur as a result of random collision of proteins, rather than formation of stable complexes, scenarios which are difficult to distinguish experimentally. Phosphorylating conditions are required to form the $CheZ_2(CheY)_2$ complex (*31*), and the resultant incorporation of CheY into $CheZ_2$ could give cross-linked oligomers if CheY had a higher tendency than $CheZ_2$ to undergo the cross-linking chemistry. In support of this possibility, CheY has a significantly higher density of surface lysine residues (reactive to cross-linkers) than CheZ and the same cross-linking reagent reacted with CheY in the absence of CheZ to give some $CheY_2$ (*18*), which is not biologically relevant and must have occurred via random collision. On the other hand, cross-linked products were not observed with several inactive CheZ mutants containing substitutions near critical residue Gln 147 but which bound to CheZ in a bead binding assay (*32*). Failure to observe cross-linking with the mutant CheZs could mean that the cross-linking assay is specific for oligomer

formation or that nonspecific cross-linking involves cross-linker-reactive groups whose exposure changes as CheZ undergoes catalytic turnover. Because of possible alternative explanations for the cross-linking experiments, the observation that CheY N59R-P does not form higher oligomers, and the demonstration here that fluorescence anisotropy experiments do not provide evidence for CheZ oligomerization, further evidence, such as direct molecular weight determination by analytical ultracentrifugation, is required to substantiate the presence of higher aggregates of $CheZ_2$-$(CheY)_2$.

ACKNOWLEDGMENT

Thanks to Bob Bourret for many helpful discussions and critical review of the manuscript, Eric Hamlett for assistance with mass spectrometry, and Dr. Jose Garcia de la Torre, University of Madrid, for assistance in the application and interpretation of the HYDROPRO software package.

REFERENCES

1. Sourjik, V. (2004) Receptor clustering and signal processing in *E. coli* chemotaxis, *Trends Microbiol. 12*, 569−576.
2. Bourret, R. B., and Stock, A. M. (2002) Molecular information processing: Lessons from bacterial chemotaxis, *J. Biol. Chem. 277*, 9625−9628.
3. Eisenbach, M. (2004) in *Chemotaxis* (Eisenbach, M., Ed.) pp 53-215, Imperial College Press, London.
4. Segall, J. E., Manson, M. D., and Berg, H. C. (1982) Signal processing times in bacterial chemotaxis, *Nature 296*, 855−857.
5. Sourjik, V., and Schmitt, R. (1998) Phosphotransfer between CheA, CheY1, and CheY2 in the chemotaxis signal transduction chain of *Rhizobium meliloti*, *Biochemistry 37*, 2327−2335.
6. Park, S.-Y., Chao, X., Gonzalez-Bonet, G., Beel, B. D., Bilwes, A. M., and Crane, B. R. (2004) Structure and function of an unusual family of protein phosphatases: the bacterial chemotaxis proteins CheC and CheX, *Mol. Cells 16*, 563−574.
7. Szurmant, H., Muff, T. J., and Ordal, G. W. (2004) CheC and FliY are members of a novel class of CheY-P-hydrolyzing proteins in the chemotactic signal transduction cascade, *J. Biol. Chem. 279*, 21787−21792.
8. Zhao, R., Collins, E. J., Bourret, R. B., and Silversmith, R. E. (2002) Structure and catalytic mechanism of the *E. coli* chemotaxis phosphatase CheZ, *Nat. Struct. Biol. 9*, 570−575.
9. Boesch, K. C., Silversmith, R. E., and Bourret, R. B. (2000) Isolation and characterization of nonchemotactic CheZ mutants of *Escherichia coli*, *J. Bacteriol. 182*, 3544−3552.
10. Stock, A. M., and Stock, J. B. (1987) Purification and characterization of the CheZ protein of bacterial chemotaxis, *J. Bacteriol. 169*, 3301−3311.
11. Bray, D., Bourret, R. B., and Simon, M. I. (1993) Computer simulation of the phosphorylation cascade controlling bacterial chemotaxis, *Mol. Biol. Cell 41*, 469−482.
12. Silversmith, R. E., Smith, J. G., Guanga, G. P., Les, J. T., and Bourret, R. B. (2001) Alteration of a nonconserved active site residue in the chemotaxis response regulator CheY affects phosphorylation and interaction with CheZ, *J. Biol. Chem. 276*, 18478−18484.
13. Appleby, J. L., and Bourret, R. B. (1998) Proposed signal transduction role for conserved CheY residue Thr87, a member of the response regulator active-site quintet, *J. Bacteriol. 180*, 3563−3569.
14. Majima, E., Goto, S., Hori, H., Shinohara, Y., Hong, Y.-M., and Terada, H. (1995) Stabilities of the fluorescent SH-reagent eosin-5-maleimide and its adducts with sulfhydryl compounds, *Biochim. Biophys. Acta 1243*, 336−342.
15. Lakowicz, J. R. (1999) *Principles of Fluorescence Spectroscopy*, 2nd ed., Kluwer Academic/Plenum Publishers, New York.
16. Weast, R. C. (1974) *CRC Handbook of Chemistry and Physics*, CRC Press, Cleveland, OH.
17. Garcia de la Torre, J., Huertas, M. L., and Carrasco, B. (2000) Calculation of hydrodynamic properties of globular proteins from their atomic-level structure, *Biophys. J. 78*, 719−730.
18. Blat, Y., and Eisenbach, M. (1996) Oligomerization of the phosphatase CheZ upon interaction with the phosphorylated form of CheY—the signal protein of bacterial chemotaxis, *J. Biol. Chem. 271*, 1226−1231.
19. Runnels, L. W., and Scarlata, S. F. (1995) Theory and application of fluorescence homotransfer to melittin oligomerization, *Biophys. J. 69*, 1569−1583.
20. Alatossava, T., Jutte, H., Kuhn, A., and Kellenberger, E. (1985) Manipulation of intracellular magnesium content in polymyxin B nonapeptide-sensitized *Escherichia coli* by ionophore A23187, *J. Bacteriol. 162*, 413−419.
21. Silver, S. (1996) *Transport of Inorganic Ions*, Vol. 1, ASM Press, Washington, D.C.
22. Silversmith, R. E., Guanga, G. P., Betts, L., Chu, C., Zhao, R., and Bourret, R. B. (2003) CheZ-mediated dephosphorylation of the *Escherichia coli* response regulator CheY: a role for CheY glutamate 89, *J. Bacteriol. 185*, 1495−1502.
23. Sourjik, V., and Berg, H. C. (2000) Localization of components of the chemotaxis machinery of *Escherichia coli* using fluorescent protein fusions, *Mol. Microbiol. 37*, 740−751.
24. Cantwell, B. J., Draheim, R. R., Weart, R. B., Nguyen, C., Stewart, R. C., and Manson, M. D. (2003) CheZ phosphatase localizes to chemoreceptor patches via CheA-short, *J. Bacteriol. 185*, 2354−2361.
25. Vaknin, A., and Berg, H. C. (2004) Single-cell FRET imaging of phosphatase activity in the *Escherichia coli* chemotaxis system, *Proc. Natl. Acad. Sci. U.S.A. 101*, 17072−17077.
26. Lipkow, K., Andrews, S., and Bray, D. (2005) Simulated diffusion of CheYp through the cytoplasm of *E. coli*, *J. Bacteriol. 187*, 45−53.
27. O'Connor, C., and Matsumura, P. (2004) The accessibility of Cys-120 in $CheA_s$ is important for the binding of CheZ and enhancement of CheZ phosphatase activity, *Biochemistry 43*, 6909−6916.
28. Li, M., and Hazelbauer, G. L. (2004) Cellular stoichiometry of the components of the chemotaxis signaling complex, *J. Bacteriol. 186*, 3687−3694.
29. McEvoy, M. M., Bren, A., Eisenbach, E., and Dahlquist, F. W. (1999) Identification of the binding interfaces on CheY for two of its targets, the phosphatase CheZ and the flagellar switch protein, FliM, *J. Mol. Biol. 289*, 1423−1433.
30. Blat, Y., Gillespie, B., Bren, A., Dahlquist, F. W., and Eisenbach, M. (1998) Regulation of phosphatase activity in bacterial chemotaxis, *J. Mol. Biol. 284*, 1191−1199.
31. Blat, Y., and Eisenbach, M. (1994) Phosphorylation-dependent binding of the chemotaxis signal molecule CheY to its phosphatase, CheZ, *Biochemistry 33*, 902−906.
32. Blat, Y., and Eisenbach, M. (1996) Mutants with defective phosphatase activity show no phosphorylation-dependent oligomerization of CheZ—the phosphatase of bacterial chemotaxis, *J. Biol. Chem. 271*, 1232−1236.

BI0501636